

A Configurational Study of Poly(vinylamine) by Multinuclear Nuclear Magnetic Resonance

C. Chang, D. D. Muccio, and T. St. Pierre*

Department of Chemistry, The University of Alabama at Birmingham, Birmingham, Alabama 35294

C. C. Chen and C. G. Overberger

Department of Chemistry and the Macromolecular Research Center, The University of Michigan, Ann Arbor, Michigan 48109. Received September 9, 1985

ABSTRACT: The tacticity of poly(vinylamine) (PVAm) prepared from *tert*-butyl *N*-vinylcarbamate (PVAmI) and from *N*-vinylacetamide (PVAmII) was determined by ^{13}C NMR. The configurational sensitivity was optimal at pH 8.8, where nine well-resolved methine carbon resonances and five methylene carbon resonances were observed. Based on the meso (*m*) and racemic (*r*) assignments for the methylene carbon resonances of PVAm made previously by the use of heteronuclear correlated 2D NMR experiments, the diad distribution for the PVAmI methylene regions was found to be 56% (*r*) and 44% (*m*). These results were extended to the tetrad analysis of the methylene peaks. The triad analysis was obtained from the relative area of the three distinct methine regions. The pentad assignments were made by a comparison of the nine methine peak areas with those calculated from first-order Markov and Bernoullian statistics. This analysis is supported, at the triad level, by ^{15}N NMR. Acetylated PVAmI, poly(*N*-vinylacetamide), was characterized by ^1H NMR for triad analysis of the COCH_3 group. This analysis gave internally consistent results with the ^{13}C analysis. A similar analysis for PVAmII gave 49% (*r*) and 51% (*m*).

Introduction

Several studies of the titration behavior of poly(vinylamine) (PVAm) have been reported, but only two reports have appeared concerning the tacticity of this polymer. Murano and Harwood¹ employed ^1H NMR to determine the tacticity of PVAmI, prepared from *tert*-butyl *N*-vinylcarbamate, indirectly by analysis of the acetyl derivative, poly(*N*-vinylacetamide) (PVAc). On the basis of the comparison of the methyl peaks of PVAc with the methyl peaks of acetylated *meso*- and *rac*-2,4-diaminopentane (DAP), they concluded that PVAmI was essentially a syndiotactic (*r* > *m*) polymer. St. Pierre et al.² investigated PVAmI by ^{13}C NMR. The assignments of the three methine peaks, *mm*, *mr*, and *rr* from low to high field, were based on the changes of chemical shift with pH and known assignments of poly(vinyl alcohol).³ According to the relative areas of the methine peaks, the polymer was judged to be atactic. An atactic polymer with opposite methine assignments, based on the relative ^{13}C chemical shift of *meso*- and *rac*-DAP, was recently reported by Chang et al.⁴

Because of the uncertainty of both the ^1H and ^{13}C peak assignments and the apparent discrepancy in tacticity, a systematic study of PVAm was undertaken. The methylene assignments for PVAm were based on ^{13}C analysis using heteronuclear correlated 2D NMR experiments and confirmed by applying the same experiments to *meso*- and *rac*-DAP.⁵ In this study the tacticity of both PVAmI and PVAmII, the latter prepared from *N*-vinylacetamide, was determined by quantitative ^{13}C and ^{15}N NMR analysis. The comparison of the two slightly different polymers was useful in confirming the peak assignments. Finally, the ^1H NMR analysis of PVAc was shown to be consistent with the ^{13}C and ^{15}N analyses of the parent polymer. Both Bernoullian and first-order Markov statistics were used for fitting and testing the experimental results.

Materials and Methods

PVAmI⁶ was prepared from *tert*-butyl *N*-vinylcarbamate, and PVAmII⁷ was prepared from *N*-vinylacetamide. PVAc⁸ was synthesized by adding acetic anhydride to a Me_2SO solution of PVA-*n*HOSu (HOSu = *N*-hydroxysuccinimide, *n* > 6) at 25 °C and isolated by precipitation in acetone. The model compounds, *meso*- and *rac*-diaminopentane (DAP), were prepared by the

method of Bosnich.⁹ The NMR spectra were recorded with a GE 300 WB spectrometer (NT series) equipped with a 1280 computer and 293c pulse programmer. The ^{13}C NMR spectra were obtained with gated decoupling (decoupler off during delay time) on 5% (w/v) solutions in D_2O at 25 °C. The repetition rate for these measurements was 10 times the longest spin-lattice relaxation time. The T_1 values were measured from the inversion-recovery pulse sequence,¹⁰ employing a composite 180° pulse with delay values of 0.01, 0.05, 0.1, 0.2, 0.5, and 1.4 s. The T_1 values were calculated by using a nonlinear, three-parameter fitting procedure.¹¹ ^{13}C NMR spectra were obtained with dioxane as an internal chemical shift reference (66.5 ppm relative to tetramethylsilane). Pulse angles of 58° (19 μs), repetition rates of 2.5 s, sweep widths of ± 7575 Hz, and 16K data points were used to acquire the free induction decays. The ^{15}N NMR spectra of PVAmI were obtained with proton decoupling and gated decoupling on 10% (w/v) solutions in 10% D_2O at 25 °C. Pulse angles of 75° (30 μs), repetition rates of 10 s, sweep widths of ± 1000 Hz, and 2K data points were used to acquire the free induction decays. The T_1 's were measured, as above, by using delay values of 0.01, 0.2, 0.7, 2.8, and 5.6 s. Nuclear Overhauser effects (NOE) were determined by the ratio of the peak intensity of the fully proton-decoupled and gated-decoupled (decoupler off during delay time) spectra. Ammonium chloride in 10 M HCl was used as an external chemical shift reference (30.31 ppm from liquid ammonia at 25 °C). ^1H NMR spectra were obtained on 0.3% (w/v) by weight in D_2O solutions with TSP as an internal reference at 25, 40, 60, and 80 °C. Curve deconvolution was accomplished with the NMCCAP program provided with the GE software using a completely Lorentzian line shape. The pHs were adjusted with NaOD and recorded on an Orion research model 701A pH meter with a microcapillary Ingold combination electrode.

Results and Discussion

The ^{13}C NMR spectra of both PVAmI and PVAmII were recorded at pH 8.8 in D_2O by using a gated-decoupled pulse sequence in order to suppress the NOE. The configurational sensitivity is optimal at this pH. As the pH is lowered, the tacticity effects disappear, leaving a single, but sharp peak for the methine carbon and a broad peak for the methylene carbon at pH 2 (Figure 1). At higher pH values, the configurational sensitivity is preserved, but the methine and methylene carbon peaks are overlapped (Figure 1). The ^{13}C NMR spectrum of PVAmI and its simulated spectrum are shown in Figure 2. Five regions, labeled A-E, are observed. The A, B, and C regions belong to the methine carbon resonances, and the D and E regions

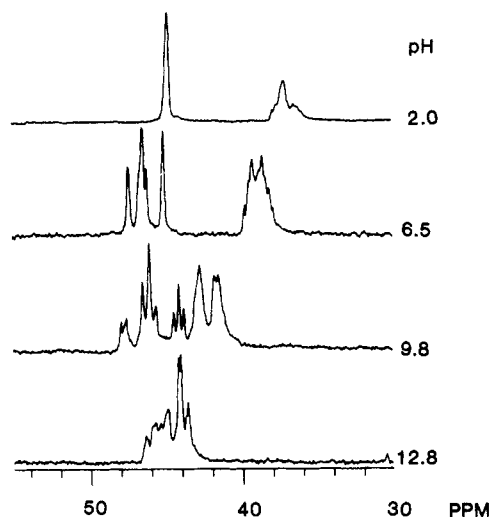


Figure 1. ^{13}C NMR of PVAmI in D_2O at 25°C and at the indicated pHs.

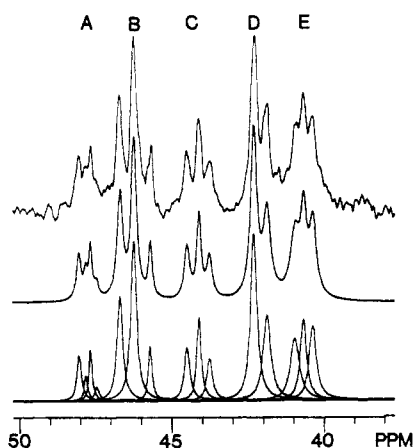


Figure 2. ^{13}C NMR of PVAmI in D_2O at 25°C and at pH 8.8 with CH_2 from 40 to 43 ppm and CH from 43 to 49 ppm. The top spectrum was observed and the middle and bottom spectra were calculated.

belong to the methylene carbon resonances. The areas of these five regions, obtained from curve deconvolution, are 17, 54, and 29% for the A, B, and C triad distribution, respectively, and 55 and 45% for D and E diad distribution, respectively.

In order to ensure a quantitative relationship between peak areas and the number of carbons, it is necessary to avoid saturation. Therefore, the T_1 values at pH 8.8 were measured and found to have almost equal values for the peaks in the methine carbon region (0.25 s) and the peaks in the methylene carbon region (0.13 s). Because nearly $10T_1$ was used for the repetition rates in the acquisition of these gated-decoupled spectra, it is not necessary to correct the peak areas.

Initially the model compounds, *meso*- and *rac*-DAP, were used to assign the diad configuration of the methylene carbon of PVAmI.⁴ The fully proton-decoupled ^{13}C NMR spectrum of a 1:2 molar mixture of *meso*- and *rac*-DAP was recorded at 25°C and pH 8.8. The observed smaller CH_2 resonance at low field (39.59 ppm) was due to the *meso* isomer and upfield resonance (39.00 ppm) due to the *racemic* isomer. These relative chemical shifts were first used to assign the *m* and *r* diads of the polymer.⁴ However, further studies employing heteronuclear correlated 2D NMR demonstrate convincingly that the D region (55%) of PVAmI must be assigned to the *r* diad and the E region (45%) to the *m* diad.

Our initial analysis assumes that all *r*- and *m*-centered peaks are grouped together in regions D and E, respectively, and likewise for the *rr*-, *mr*-, and *mm*-centered peaks. Bernoullian statistics^{12,13} were employed to test the triad sequence from these *r* and *m* probabilities, which gave 30, 50.5, and 20.5% for the *rr*-, *mr*-, and *mm*-triad sequences, respectively. A comparison of the calculated and experimental values for the triad analysis led to the tentative assignment of the *mm* sequence to the A region and the *rr* sequence to the C region. The experimental values for the three methine peaks were used to calculate the diad sequence, 56% (*r*) and 43% (*m*), according to Bernoullian statistics.¹⁴ First-order Markov statistics were also used to fit the experimental results from the methine triad regions by the following relations:¹³

$$P_{m/r} = (mr) / [2(mm) + (mr)]$$

$$P_{r/m} = (mr) / [2(rr) + (mr)]$$

$$P_m = P_{r/m} / (P_{m/r} + P_{r/m})$$

$$P_r = P_{m/r} / (P_{m/r} + P_{r/m})$$

These calculations gave the diad sequence 56% (*r*) and 44% (*m*). These two different statistics gave similar diad distributions and values close to the experimental values of D and E.

The methine carbon appeared as nine peaks, suggesting pentad resolution. Based on either Bernoullian or first-order Markov statistics, these calculated pentad values were compared to the experimental results. On the basis of matched areas, the high-order assignments were made. Experimental and calculated pentad distributions with assignments and chemical shifts are given in Table I. Since the *rr*-centered peaks were better resolved, they were examined by both Bernoullian and first-order Markov statistics. Using this more critical test, we found little difference between these statistics, as expected for atactic polymers. Because the probabilities of *rrrr*-, *mrrm*-, *mrrr*-, *rrmm*-, *rmrm*-, and *mmmm*- are very different, within their respective triads, their assignments were made with confidence (Table I). For instance, if the positions of *rrrr* and *mrrm* were interchanged, a significantly poorer fit was observed. As to the *mr*-centered triad (Table I), suggested assignments are made but with less confidence. The standard deviation between calculated and experimental results was 1.1% for the first-order Markov statistics and 1.7% for the Bernoullian statistics.

The methylene carbon consists of five peaks, suggesting a tetrad resolution. Comparing the calculated tetrad sequences to the experimental results, it is obvious that the sequences cannot be assigned unambiguously. As mentioned above, the D region was assigned to the *r* diad; however, it is also possible to have an *m*-centered resonance contribute to the D region and vice versa, as reported by Ovenall for poly(vinyl alcohol).¹⁵ We find in particular a better fit might be obtained for the tetrad data by interchanging the *rrr* and *rmr* contributions to the D and E regions (Table I), but on the basis of our 2D results⁵ the peak at 41.89 ppm belongs to an *r*-centered tetrad.

The tacticity of PVAmII was also analyzed by this procedure, and the results are shown in Table I. This analysis gave 49% (*r*) and 51% (*m*) for PVAmII based on first-order Markov statistics. Although PVAmI and PVAmII did not have sufficiently different tacticities at the diad level, they exhibited larger differences at the triad and pentad level. For example, *rrrr* and *mmmm* for PVAmII decreased and increased, respectively, according to the slight changes in *r* and *m* values between the two polymers (Table I).

Table I
¹³C NMR Analysis of Poly(vinylamine)

peak assignment	δ	PVAmI			PVAmII		
		first order	zero order ^a	exptl ^b	first order	zero order ^a	exptl ^b
<i>r</i>		0.56		0.55	0.50		0.48
<i>m</i>		0.44		0.45	0.50		0.52
<i>rr</i>				0.29			0.23
<i>mr</i>				0.54			0.54
<i>mm</i>				0.17			0.23
<i>mmm</i>	40.40	0.07	0.09	0.10	0.10	0.13	0.11
<i>mmr</i>	40.67	0.21	0.22	0.21	0.25	0.25	0.31
<i>rmr</i>	40.97	0.17	0.14	0.15	0.15	0.12	0.10
<i>rrr</i>	41.89	0.15	0.17	0.16	0.10	0.12	0.14
<i>mrr</i>	42.29	0.28	0.28	0.39	0.25	0.25	0.40
<i>mrmm</i>		0.13	0.11		0.15	0.13	
<i>mrrm</i>	43.75	0.07	0.06	0.07	0.07	0.06	0.07
<i>mrrr</i>	44.10	0.14	0.15	0.14	0.11	0.12	0.11
<i>rrrr</i>	44.50	0.08	0.10	0.08	0.05	0.06	0.05
<i>mrmm</i>	45.67	0.10	0.10	0.07	0.14	0.13	0.11
<i>mmrr</i>		0.11	0.12		0.11	0.13	
<i>rmrm</i>	46.22	0.16	0.12	0.30	0.16	0.13	0.29
<i>rrmr</i>	46.70	0.17	0.15	0.18	0.13	0.12	0.14
<i>mmmm</i>	47.43	0.03	0.04	0.02	0.05	0.07	0.05
<i>mmmr</i> ^c	47.73	0.08	0.10	0.09	0.12	0.13	0.11
<i>rmmr</i>	48.03	0.06	0.06	0.06	0.07	0.06	0.07

^a Bernoullian. ^b Based on $S/N \approx 20$, the error is estimated to be $\pm 5\%$. ^c Notice in Figure 2 that region A consists of four peaks instead of the expected three peaks. Counting from left to right, peaks 2 and 3 were combined in this assignment.

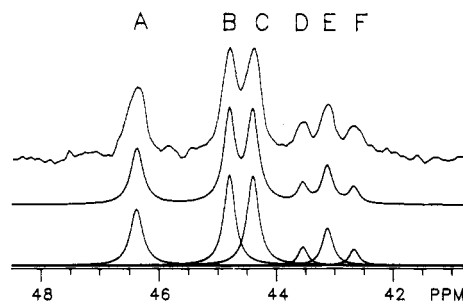


Figure 3. ¹⁵N NMR of PVAmI in 10% D₂O at 25 °C and at pH 10.5. The top spectrum was observed and the middle and bottom were calculated.

In addition to the ¹³C results, we have used ¹⁵N NMR to determine the tacticity of PVAm. The ¹⁵N NMR spectrum of PVAmI in 10% D₂O at 25 °C and its simulated spectrum are shown in Figure 3. Well-resolved peaks at 46.5, 44.7, 44.2, 43.4, 42.9, and 42.4 ppm were observed, labeled A–F, respectively. The T_1 values of these six peaks were found to be almost equal (1.0 ± 0.1 s). The NOE of peak A is -3.7 ± 0.1 , that of peaks B and C is -3.5 ± 0.1 , and that of peaks D, E, and F is -2.8 ± 0.1 . The areas of these six peaks obtained with NOE (better sensitivity than without NOE) are 20, 29, 29, 5, 12, and 5% for peaks A–F, respectively. After normalization for NOE, the respective areas of these six peaks are 18, 28, 29, 6, 14, and 6%. On the basis of the triad distribution obtained from the ¹³C NMR results, we assign the A peak as the *mm* triad (18%), the B and C peaks as the *mr* triad (56%), and the D, E, and F peaks as the *rr* triad (26%). It is worth noting that the *rr* triad shows pentad sensitivity in the ¹⁵N spectrum (Figure 3) as detected in the ¹³C results (Figure 2). The assignments of the *rr*-centered peaks for ¹⁵N NMR are the same as for the ¹³C NMR results, based on both relative areas.

In order to link this work with the earlier study of Murano and Harwood,¹ the ¹H NMR analysis of PVAm was undertaken. Unlike poly(acrylic acid),¹⁶ the methylene proton resonances of PVAm are not resolved at any pH. Therefore, the tacticity of PVAc, acetylated from PVAmI,

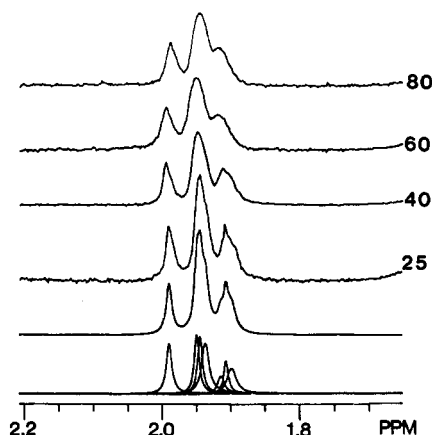


Figure 4. ¹H NMR of PVAc in D₂O at the indicated temperatures (°C) for CH₃ only. The bottom two spectra were calculated from deconvolution.

was determined by ¹H NMR assuming that PVAc and the parent polymer have the same tacticity. As first reported by Murano and Harwood, the ¹H NMR of PVAc at 100 °C is expected to provide a triad analysis which would complement our ¹³C analysis. The ¹H NMR spectra of the methyl peaks for PVAc at different temperatures, 25, 40, 60, and 80 °C at pH 2 are shown in Figure 4. Clearly, the resolution for triad sensitivity was better at 25 °C. The peak areas obtained from curve deconvolution for the three triad peaks are 16.0, 55.3, and 28.7%, ordered low to high field. Compared to the ¹³C and ¹⁵N triad results of PVAmI (Table I), the assignments of PVAc for the methyl protons are *mm*, *mr*, and *rr* from low field to high field.

It is clear from these results that (1) the ¹³C NMR of PVAm solutions adjusted to pH 8–9 provides useful information concerning sequence distribution at the diad and triad level and at higher levels with curve deconvolution, (2) the PVAm sequence distribution is close to random but detectably different, depending on whether the polymer was prepared from *N*-vinylacetamide or *tert*-butyl *N*-vinylcarbamate, and (3) ¹⁵N NMR may also be used to analyze the sequence distribution of PVAm. It should also

be noted that the ^1H NMR of the acetylated PVAm provides corroborating evidence for the triad analysis of PVAm, and the configurational analysis of the latter is consistent with the configurational analysis of poly(vinyl alcohol).

Registry No. *meso*-DAP, 29745-96-8; *rac*-DAP, 29745-97-9.

References and Notes

- (1) Murano, M.; Harwood, H. J. *Macromolecules* **1970**, *3*, 605.
- (2) St. Pierre, T.; Lewis, E. A.; Levy, G. C. In "Polymeric Amines and Ammonium Salts"; Goethals, E. T., Ed.; Pergamon Press: Oxford, 1980; pp 245-248.
- (3) Wu, T. K.; Ovenall, D. W. *Macromolecules* **1973**, *6*, 582.
- (4) Chang, C.; Muccio, D. D.; St. Pierre, T.; Chen, C. C.; Overberger, C. G. *Polym. Prepr., Am. Chem. Soc., Div. Polym. Chem.* **1985**, *26* (2), 265.
- (5) Chang, C.; Muccio, D. D.; St. Pierre, T. *Macromolecules* **1985**, *18*, 2334.
- (6) Hughes, A. R.; St. Pierre, T. In "Macromolecular Synthesis"; Mulvaney, J. E., Ed.; Wiley: New York, 1977; pp 31-37.
- (7) Dawson, D. J.; Gless, R. D.; Wingard, R. E., Jr. *J. Am. Chem. Soc.* **1976**, *98*, 5996.
- (8) Overberger, C. G.; Chen, C. C. *J. Polym. Sci., Polym. Lett. Ed.* **1985**, *23*, 345.
- (9) Bosnich, B.; Harrowfield, J. M. *J. Am. Chem. Soc.* **1972**, *94*, 3425.
- (10) Freeman, R.; Kempell, S. P.; Levitt, M. H. *J. Magn. Reson.* **1980**, *38*, 453.
- (11) Kowalewski, J.; Levy, G. C.; Johnson, L. F.; Palmer, L. J. *Magn. Reson.* **1977**, *26*, 533.
- (12) Randall, J. "Polymer Sequence Determination: ^{13}C NMR Method"; Academic Press: New York, 1977; p 71.
- (13) Bovey, F. A. In "High Resolution NMR of Macromolecules"; Bower, D. J., Ed.; Academic Press: New York, 1972; p 146.
- (14) The best values were calculated by a linear regression of the log form of $(m)^2 = 0.288$, $2(mr) = 0.541$, and $(r)^2 = 0.171$.
- (15) Ovenall, D. W. *Macromolecules* **1983**, *17*, 1458.
- (16) Chang, C.; Muccio, D. D.; St. Pierre, T. *Macromolecules* **1985**, *18*, 2154.

Photochemical Cleavage of a Polymeric Solid: Details of the Ultraviolet Laser Ablation of Poly(methyl methacrylate) at 193 and 248 nm

R. Srinivasan,* B. Braren, D. E. Seeger, and R. W. Dreyfus

IBM T. J. Watson Research Center, Yorktown Heights, New York 10598.

Received October 18, 1985

ABSTRACT: The products of the laser ablation of poly(methyl methacrylate) (PMMA) ($\bar{M}_n \sim 800\,000$) at 193 or 248 nm range from C_2 through methyl methacrylate (MMA) and a solid that is a low molecular weight ($\bar{M}_n = 2500$) fraction of PMMA. While the products are the same at both wavelengths, the mix is quite different. At 193 nm, 18% of the ablated polymer is MMA, whereas at 248 nm less than 1% of the polymer appeared as MMA. A semilogarithmic plot of the mass of material removed vs. the fluence shows three distinct regions. The central portion at each wavelength (80-300 mJ/cm² at 193 nm, 600-2000 mJ/cm² at 248 nm), which corresponds to rapid etching, is identified as "ablative photodecomposition". At lower fluences, the etching efficiency falls off rapidly, indicating that there is a threshold fluence. At fluences above the range for ablative photodecomposition, the etching levels off, probably due to the secondary absorption of the incoming photons by the products. The formation of C_2 as a product was monitored by laser-induced fluorescence. The velocity distribution of the product as a function of fluence was also measured. The velocity distribution approaches but does not exactly fit a Maxwell-Boltzmann equation. Average translational energies as high as 6 eV were recorded even at the fluence threshold for this product. It is suggested that ablative photodecomposition involves both a one-photon process, which produces MMA and low molecular weight polymeric fragments, and a multiphoton process, which gives rise to products such as C_2 with high translational energy. At longer wavelengths, a greater temperature rise within the ablated volume may be necessary to increase the quantum yield for bond-breaking. The mass of material ablated per joule of energy absorbed in the ablated volume was remarkably similar at both wavelengths. Ablative photodecomposition is a novel method to cleave an organic solid. In contrast to alternative methods such as mechanical pressure or thermal decomposition, both of which occur in the ground electronic state of the bonds undergoing rupture, ablative photodecomposition involves the electronically excited state of the bond that is broken. It may therefore limit secondary effects of the cleavage to a highly localized region, a feature that can be of considerable interest in living systems.

Introduction

In a series of recent articles¹⁻⁵ we and others showed that the action of ultraviolet laser radiation causes the breakup and spontaneous removal of material from the surface of an organic polymeric solid by a process that we have termed "ablative photodecomposition". Over an area that is defined by the light beam, the surface of the solid is etched away to a depth of 0.1-4 μ at every pulse, and the products are expelled at supersonic velocity.^{6,7} Most of the publications have been concerned with the physical and applied aspects of the removal of material. Less attention has been paid to the microscopic nature of the bond-breaking that must be fundamental to the decomposition of the polymer before ablation can occur. In this article, we are concerned with the details of the chemical process

by which photon energy causes bonds to break and results in ablation of the products. This investigation also brings up a novel aspect of the cleavage of an organic solid by a beam of photons. It will be argued that thermal energy, which can break up a solid, and mechanical force, which can also cleave a solid, are processes in the ground electronic state of a bond whereas ablative photodecomposition causes the cleavage of a solid from an electronically excited state of the bonds. It may therefore constitute a very localized process that would result in a minimum of disruption of the structure of the solid.

Experimental Section

Materials. A 650- μm -thick commercial PMMA sheet ($\bar{M}_n \sim 800\,000$) was used in all of the determinations of etch depth as a function of fluence. Scanning electron microscopy (SEM) of